

# Mass and radius constraints for neutron stars from pulse shape modeling

Tuomo Salmi

University of Turku

*thjsal@utu.fi*

November 15, 2016

- Determination of masses and radii for rapidly rotating neutron stars
- Constrain the number of possible equations of state
- The properties of matter at extremely high densities
- Study the effects of polarization measurements on mass and radius constraints

- Introduction
  - Neutron stars
  - Accreting millisecond pulsars
- Methods
  - Modeling the pulse profiles of accreting millisecond pulsars
  - Bayesian inference and Monte Carlo sampling methods
  - Test our tools and methods with synthetic data
- Results
  - Polarization measurements may be used to get significantly tighter constraints for masses and radii.

# Neutron stars

- Most dense objects that can be directly observed
- Typical mass  $M = 1.5M_{\odot}$  and typical radius  $R = 12$  km
- Supernuclear densities (5 to 10 times the nuclear equilibrium density  $n_0 \approx 0.16 \text{ fm}^{-3}$  of neutrons and protons)
- Are created after the gravitational collapse of a core of a massive star ( $> 8M_{\odot}$ ) at the end of its life.

# Neutron stars

- Composition of the innermost core is unknown.
- Equation of state (EOS) gives the relation between the pressure and density (or mass and radius).
- The EOS of a neutron star is unknown.

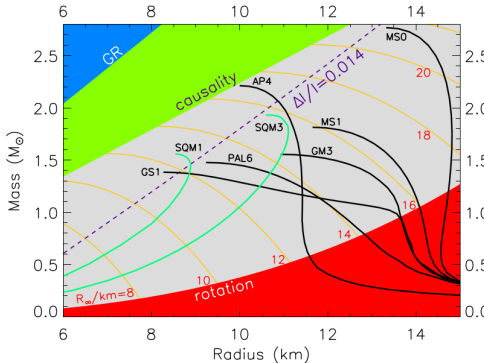


**Figure :** Figure 2 from Lattimer and Prakash (2004).

# Neutron stars

- Observed masses and radii constrain the number of possible EOSs.
- Upper limits for compactness
  - The general relativity (Schwarzschild condition)
  - Causality condition
- Lower limit for compactness
  - Fastest observed rotational frequency

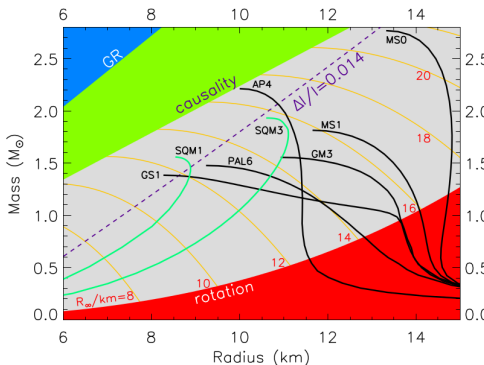


Figure : Figure 2 from Lattimer and Prakash (2004).

# Neutron stars

- The highest observed mass rules out many EOSs.
- We aim to find out independent knowledge of both mass and radius.

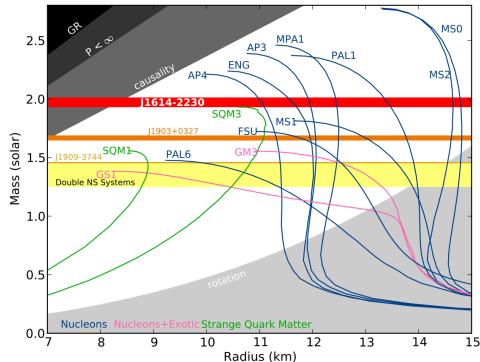


Figure : Figure from Demorest et al. (2010).

# Accreting millisecond X-ray pulsars (AMXP)

- A subgroup of low mass X-ray binaries (LMXB)
- Gas from the accretion disk (stripped from the companion) is channeled onto the magnetic poles of a millisecond pulsar.
- A pair of "hot spots"

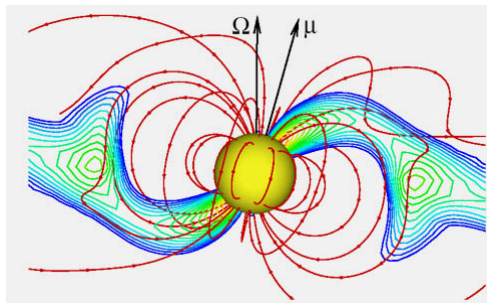


Figure : Figure 4 from Romanova et. al (2004).



# Accreting millisecond X-ray pulsars (AMXP)

- Recycling scenario
  - The evolutionary progenitors of recycled radio millisecond pulsars

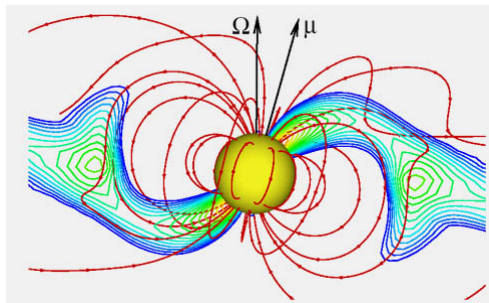


Figure : Figure 4 from Romanova et. al (2004).

# Accreting millisecond X-ray pulsars (AMXP)

- Some of AMXPs show outbursts
- SAX J1808.4–3658: Nearly coherent oscillations detected during outbursts
- Similar outburst evolution: SAX J1748.9–2021 (in the Figure)

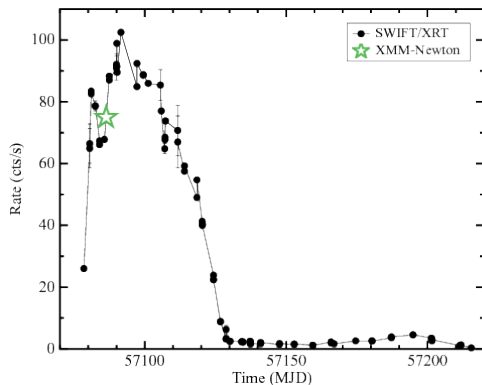
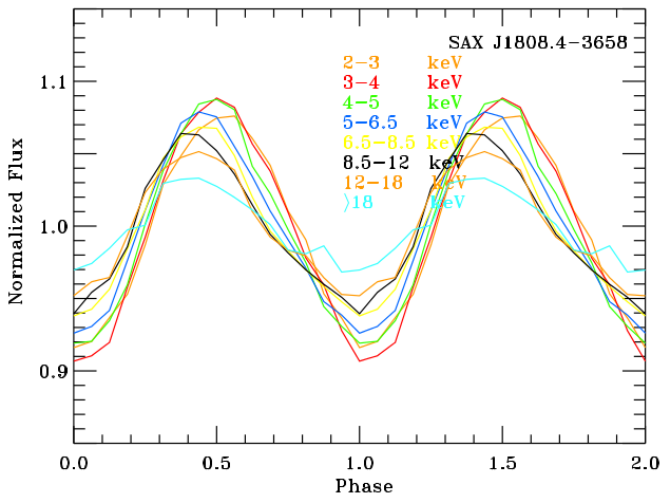


Figure : Figure 1 from Sanna et al. (2016).

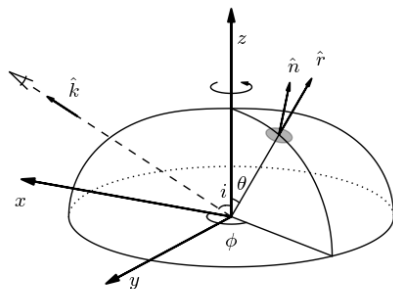
# SAX J1808.4–3658



- Pulse shape modeling
- Bayesian analysis
- Monte Carlo sampling methods

# Pulse profile modeling

- Schwarzschild + Doppler approximation (S+D)
- Oblate shape of the star taken into account
- Mass and radius affecting the light bending
- Time delays different from different locations



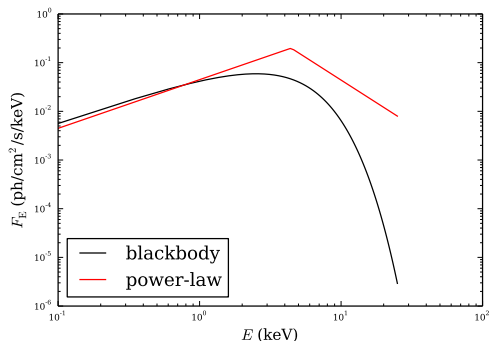
- Observed spectral flux from an infinitesimal spot:

$$dF_E = (1 - u)^{1/2} \delta^4 I'_{E'}(\sigma') \cos \sigma \frac{d \cos \alpha}{d \cos \psi} \frac{dS'}{D^2} \quad (1)$$

- $D$  = distance,  $\psi$  = bending angle,  $\delta$  = Doppler factor,  $(1 - u)^{1/2}$  = inverse of gravitational redshift,  $\sigma$  = emission angle relative to the spot normal, and  $\alpha$  = emission angle relative to the radius vector.
- Integration over the spot surface

# Pulse profile modeling

- Energy spectrum (energy dependency of  $I'_{E'}$ )
- Blackbody + Power-law according to observations
- Heated hot spot + Comptonization from an accretion shock
- In this thesis two-component power-law
- $I'_{E'}(\sigma') \propto \sigma'$  either isotropic or "Hopf" profile



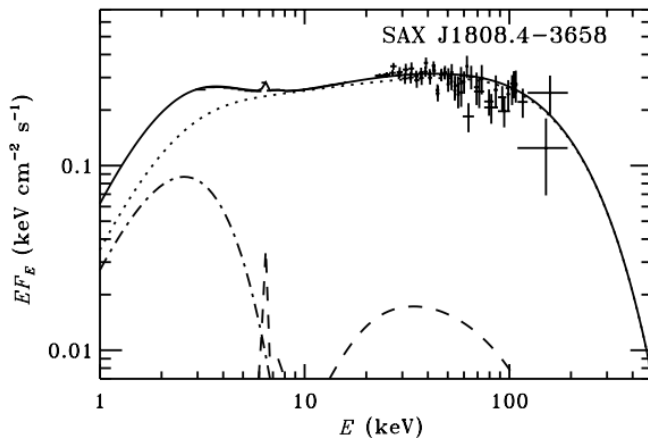


Figure : Figure 3 from Poutanen and Gierlinski (2003).



$$p(\mathbf{y}|\mathcal{D}) \propto p(\mathcal{D}|\mathbf{y})p(\mathbf{y}) \quad (2)$$

- $\mathcal{D}$  = Data
- $\mathbf{y}$  = Parameters of the pulse profile model
- $p(\mathbf{y})$  = Prior probability distributions of the parameters
- $p(\mathcal{D}|\mathbf{y})$  = Probability distribution of the data given the parameters
- $p(\mathbf{y}|\mathcal{D})$  = Probability distribution of the parameters given the data

# Ensemble sampler

- Independent walkers moving the parameter space
- Stretch-move algorithm instead of Metropolis-Hastings
- New sample is either accepted or rejected with a certain probability

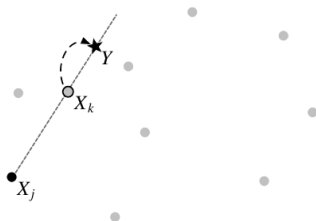


Figure : Figure 2 from Goodman and Weare (2010).

- Synthetic data
- Posterior probability distributions

- We have generated a synthetic data similar to SAX J1808.4–3658 using the pulse profile model.
- Parameters assumed to be physically reasonable
- The variability amplitude  $A$  determined mainly by observer inclination  $i$  and spot co-latitude  $\theta_s$ :

$$A = \frac{F_{\max} - F_{\min}}{F_{\max} + F_{\min}} \quad (3)$$

$$A \approx \frac{(1 - r_s/R) \sin i \sin \theta_s}{r_s/R + (1 - r_s/R) \cos i \cos \theta_s}. \quad (4)$$

$$A \approx \frac{(1 - r_s/R) \sin i \sin \theta_s}{r_s/R + (1 - r_s/R) \cos i \cos \theta_s}. \quad (5)$$

- Switching  $i$  and  $\theta_s$  has no effect on  $A$ .
- However, the variability of polarized flux depends on  $i$  and  $\theta_s$  separately.
- To study this, we have created two datasets which differ only in  $i$  and  $\theta_s$ .
- We assume either uniform or non-uniform prior probability distributions for parameters.
- We obtain posterior probability distributions for the parameters using the ensemble sampler.

Table : Parameters of the synthetic datasets.

Parameter	Value
Radius $R$	12.0 km
Mass $M$	$1.5 M_{\odot}$
Inclination $i$	$5^{\circ}$ or $75^{\circ}$
Spot colatitude $\theta_s$	$75^{\circ}$ or $5^{\circ}$
Spot angular size $\rho$	$10.0^{\circ}$
Distance $D$	2.5 kpc
Temperature $T_{\text{eff}}$	2.0 keV

# Synthetic data

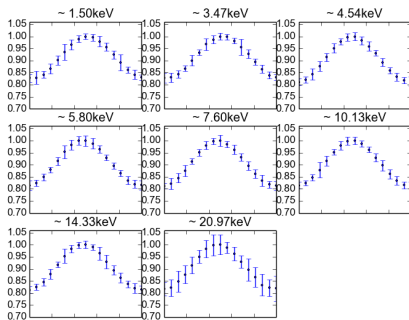


Figure : Equatorial spot

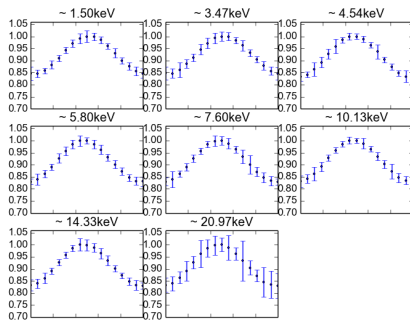


Figure : Polar spot

# Posterior probability distributions

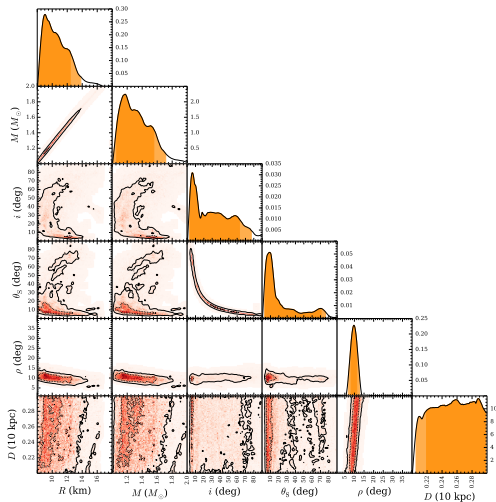


Figure : Polar spot with only uniform priors.



# Posterior probability distributions

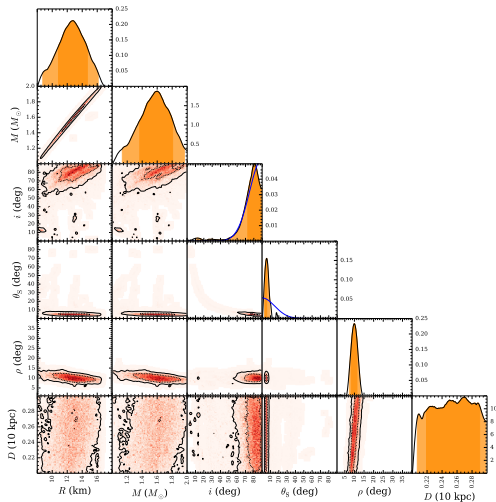


Figure : Polar spot with non-uniform  $i$  and  $\theta_s$  priors (blue lines).

# Posterior probability distributions

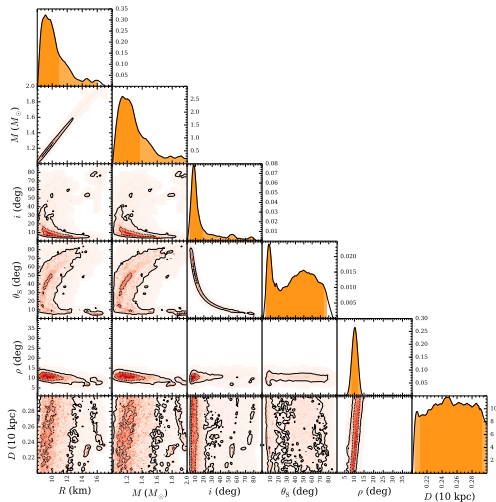


Figure : Equatorial spot with only uniform priors.

# Posterior probability distributions

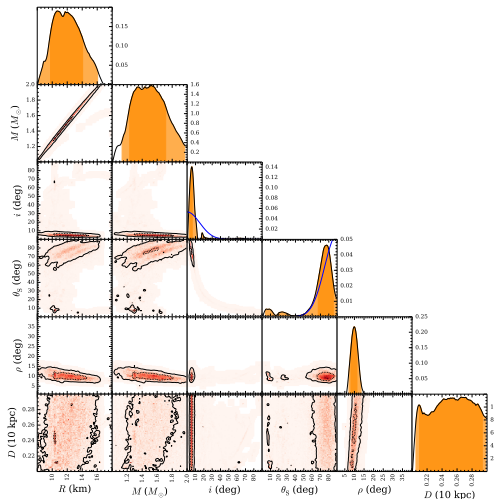


Figure : Equatorial spot with non-uniform  $i$  and  $\theta_s$  priors (blue lines).

- Only upper limits for masses and radii when only non-uniform priors
- Both upper and lower limits when prior information for  $i$  and  $\theta_s$  applied
- Correct  $i - \theta_s$  solution not found without prior information.
- The size of the spot is well constrained but the distance is not.

- AMXPs show coherent oscillations at the spinning frequency of the pulsar.
- These oscillations may be used to constrain masses and radii of pulsars.
- Tighter constraints for mass and radius from polarization
- Future
  - Develop the model
  - From synthetic to real observations

# The End